A phase-domain readout circuit for a CMOS-compatible thermal-conductivity-based carbon dioxide sensor

Cai, Zeyu; van Veldhoven, Robert; Suy, Hilco; De Graaf, Ger; Makinwa, Kofi A.A.; Pertijs, Michiel

Citation (APA)
Cai, Z., van Veldhoven, R., Suy, H., De Graaf, G., Makinwa, K. A. A., & Pertijs, M. (2018). A phase-domain readout circuit for a CMOS-compatible thermal-conductivity-based carbon dioxide sensor. In L. C. Fujino (Ed.), *2018 IEEE International Solid-State Circuits Conference, ISSCC 2018: Digest of Technical Papers* (Vol. 61, pp. 332-334). IEEE. https://doi.org/10.1109/ISSCC.2018.8310319

Important note
To cite this publication, please use the final published version (if applicable).
Please check the document version above.

19.8 A Phase-Domain Readout Circuit for a CMOS-Compatible Thermal-Conductivity-Based Carbon Dioxide Sensor

Zeyu Cai[1,2], Robert van Veldhoven[2], Hilco Suy[3], Ger de Graaf[1], Kofi A. A. Makinwa[1], Michiel Pertijs[1]

[1]Delft University of Technology, Delft, The Netherlands
[2]NXP Semiconductors, Eindhoven, The Netherlands
[3]ams AG, Eindhoven, The Netherlands

The measurement of carbon-dioxide (CO_2) concentration is very important in home and building automation, e.g. to control ventilation in energy-efficient buildings. This application requires compact, low-cost sensors that can measure CO_2 concentration with a resolution of <200 ppm over a 2500ppm range. Conventional optical (NDIR-based) CO_2 sensors require components that are CMOS-incompatible, difficult to miniaturize and power-hungry [1]. Due to their CMOS compatibility, thermal-conductivity-based sensors are an attractive alternative [2,3]. They exploit the fact that the thermal conductivity (TC) of CO_2 is lower than that of the other constituents of air, so that CO_2 concentration can be indirectly measured via the heat loss of a hot wire to ambient. However, this approach requires the detection of very small changes in TC (0.25 ppm per ppm CO_2 [3]).

This paper presents a TC-based CO_2 sensor that achieves a resolution of 94ppm (rms) while dissipating only 12mJ per measurement, >10× less than prior CMOS-compatible CO_2 sensors [3]. This is achieved by using a high-resolution phase-domain $\Delta\Sigma$ modulator (PD$\Delta\Sigma$M) to sense the thermal time constant τ_{th} of a hot wire. The time constant can be approximated by the product of the wire's thermal capacitance (C_{th}) and its thermal resistance to ambient (R_{th}). Since the wire loses part of its heat to the surrounding air, R_{th} depends on the TC of the air, and thus on CO_2 concentration (Fig. 19.8.1), while C_{th} can be considered constant. Driving the wire with periodic heat pulses then results in phase-shifted temperature variations $\Delta T(t)$, which are digitized by the PD$\Delta\Sigma$M, and from which τ_{th} can be derived [4, 5]. To maximize the sensitivity of the detected phase shift to τ_{th}, the wire is driven at $f_{drive} = 1/2\pi\tau_{th} = 9.26$kHz, i.e. at the pole of the thermal filter. Compared to measuring the steady-state temperature of a hot wire [3], this approach has the important advantage that the absolute temperature and power levels of the transducer do not need to be accurately stabilized or measured. In contrast with earlier TC sensors based on transient measurements [2,4], which use separate heaters and temperature sensors, we combine these two functions in a single resistive transducer. This greatly simplifies fabrication, because only one extra etch step is required to realize a tungsten hot-wire transducer in the via layer of a standard CMOS process [3].

To produce heat pulses at a frequency f_{drive}, the hot wire is driven by a pulsed current I_d (2.5mA). Since its resistance $R(t)$ is temperature dependent, the resulting temperature variations $\Delta T(t)$ can then be sensed via the corresponding resistance changes $\Delta R(t)$ in the hot wire. To sense $R(t)$ independently of the switched drive current I_d, an additional sense current I_s (0.5 mA), switched at $f_{sense} = 15f_{drive}$, produces a modulated voltage that is proportional to $R(t) = R_0(1+\alpha\Delta T)$, where $\alpha = 0.4\%/°C$ for tungsten, and thus has a constant sensitivity to $\Delta T(t)$ (Fig. 19.8.2, left). To ease the detection of this voltage in the presence of the large voltage transients at f_{drive} (~ 300mV$_{pp}$), two identical transducers (R_{t1} and R_{t2}) are heated simultaneously and read out differentially via out-of-phase sense currents. Thus, the signal at f_{drive} is converted into a common-mode signal that can be rejected, while the differential signal is demodulated using a chopper switch (Fig. 19.8.2, middle).

Even with this arrangement, the subsequent readout circuit must still have a large dynamic range. This is because the temperature-induced resistance change ΔR (~3Ω) is small compared to the baseline resistance R_0 (~110Ω), while the change in ΔR due to changes in CO_2 concentration is even smaller (~1.5μΩ per ppm CO_2). To cancel the voltage steps associated with R_0, two poly resistors $R_{p1,2}$ (~R_0) are connected in series with the transducers, and the sense currents are routed such that the additional voltage drop I_sR_p cancels out I_sR_0 (Fig. 19.8.2, right). The remaining differential signal V_s is ideally equal to $I_s\Delta R$ (~1.5mV$_{pp}$, 200× smaller than the initial transients), and is thus proportional to $\Delta T(t)$. However, the mismatch between the transducers and the poly resistors leads to ripple. To

minimize this, the drive and sense currents can be trimmed using three 6b current-trimming DACs with an LSB of 0.4%I_s (not shown), thus reducing the residual ripple to < 0.1mV.

To detect the CO_2-dependent changes in τ_{th}, the phase shift of ΔR relative to f_{drive} is digitized by a PD$\Delta\Sigma$M similar to [5] (Fig. 19.8.3). Rather than directly demodulating the sense voltage, as in Fig. 19.8.2, it is first converted into a current by a transconductor g_m and then detected by a chopper demodulator, resulting in a signal proportional to ΔR. A second chopper then multiplies this signal by a phase reference (a phase-shifted version of f_{drive}), resulting in a signal of which the DC component is proportional to their phase difference. This difference is integrated and quantized by a comparator clocked at $f_{samp} = f_{drive}$ to form a $\Delta\Sigma$ loop in which the bit-stream output bs switches between two phase references ϕ_0 and ϕ_1 ($\phi_0 - \phi_1 = 4°$). This loop nulls the integrator's average input, thus ensuring that the average reference phase tracks the phase of $\Delta T(t)$, which can therefore be derived from the bit-stream average. To simplify the circuit, the two choppers at the output of the transconductor have been merged into a single chopper, which is driven by the logical product of f_{sense} and the chosen phase reference.

Both the transducers and the readout circuit have been implemented in the same 0.16μm CMOS technology (Fig. 19.8.7), with active areas of 0.3mm² and 3.14mm², respectively. For flexibility, they have been realized on separate chips and connected at the PCB level, and so they can be readily co-integrated. The modulator control signals were generated using an FPGA. The readout circuit consumes 6.8mW from a 1.8V supply, 6.3mW of which is dissipated in the transducers. Fig. 19.8.4 shows the measured resolution at different oversampling ratios (OSR). A resolution equivalent to 94ppm CO_2 is reached at an OSR of 16384, which corresponds to a measurement time of 1.8s, and an energy consumption of 12mJ. The measured phase shift as a function of the drive frequency, measured using a larger full scale $\phi_0 - \phi_1 = 12°$ for clarity, shows the first-order behaviour associated with the hot wire thermal time constant.

To measure its CO_2 response, the sensor was placed in a sealed box along with an NDIR reference CO_2 sensor [1]. Like other TC-based CO_2 sensors [2,3], the readings of the sensor are affected by variations in ambient conditions, which need to be compensated in a final product. In our experiment, ambient temperature, humidity and pressure sensors were placed in the box to facilitate cross-sensitivity compensation. Figure 19.8.5 shows the good agreement between the readings of our sensor and the CO_2 concentration measured by the reference sensor.

Figure 19.8.6 summarizes the performance of the chip and compares it with the prior art. By using a low-noise phase-domain $\Delta\Sigma$ modulator and substantially reducing the required dynamic range using differential sensing and baseline compensation, this work achieves the lowest energy consumption per measurement, while using a transducer fabricated in standard CMOS technology with minimum post-processing. This results in a fully integrated CO_2 sensor in only ~3mm², making it a promising candidate for CO_2 sensing in cost- and energy-constrained applications.

References:
[1] SenseAir K30 datasheet, SenseAir [Online].
Available: http://www.senseair.com/.
[2] K. Kliche, et al., "Sensor for Thermal Gas Analysis Based on Micromachined Silicon-Microwires," *IEEE Sensors J.*, vol. 13, no. 7, pp. 2626–2635, July 2013.
[3] Z. Cai, et al., "A Ratiometric Readout Circuit for Thermal-Conductivity-Based Resistive CO_2 Sensors," *IEEE JSSC*, vol. 51, no. 10, pp. 2463-2474, Oct. 2016.
[4] C. van Vroonhoven, et al., "Phase Readout of Thermal Conductivity-Based Gas Sensors," *IEEE Int. Workshop on Advances in Sensors and Interfaces (IWASI)*, pp. 199-202, 2011.
[5] S. M. Kashmiri, et al., "A Scaled Thermal-Diffusivity-Based 16 MHz Frequency Reference in 0.16 μm CMOS," *IEEE JSSC*, vol. 47, no. 7, pp. 1535-1545, July 2012.
[6] T.A. Vincent and J.W. Gardner, "A Low Cost MEMS Based NDIR System for the Monitoring of Carbon Dioxide in Breath Analysis at ppm Levels," *Sens. and Actuators B, Chem.*, *(Elsevier)*, vol. 236, pp. 954-964, Nov. 2016.
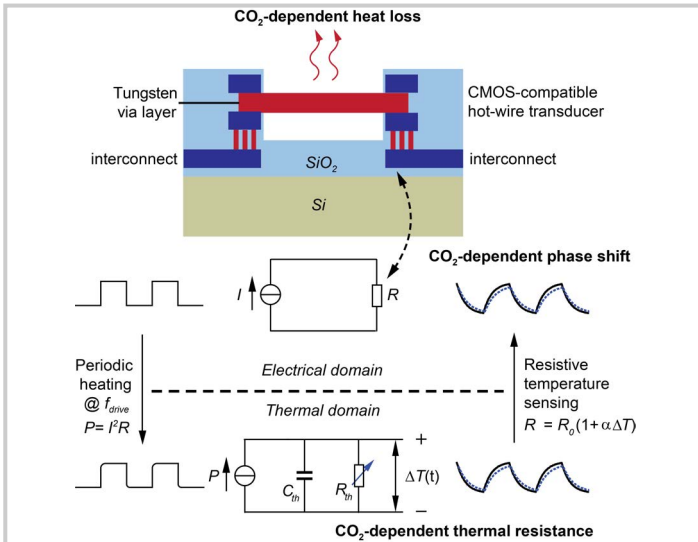
Figure 19.8.1: Transient thermal-resistance (thermal time-constant) measurement principle.
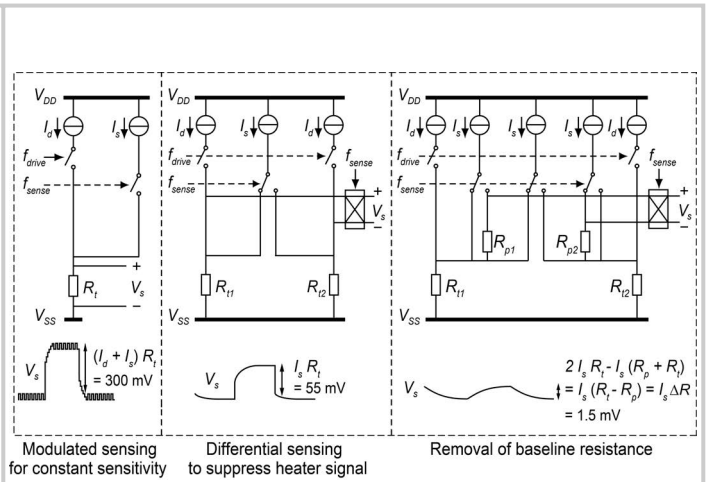

Figure 19.8.2: Sensing the temperature-induced resistance changes using modulation, differential sensing and baseline cancellation.
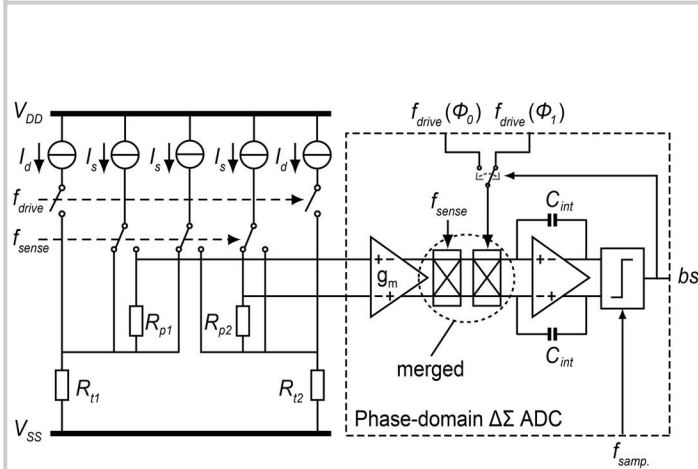

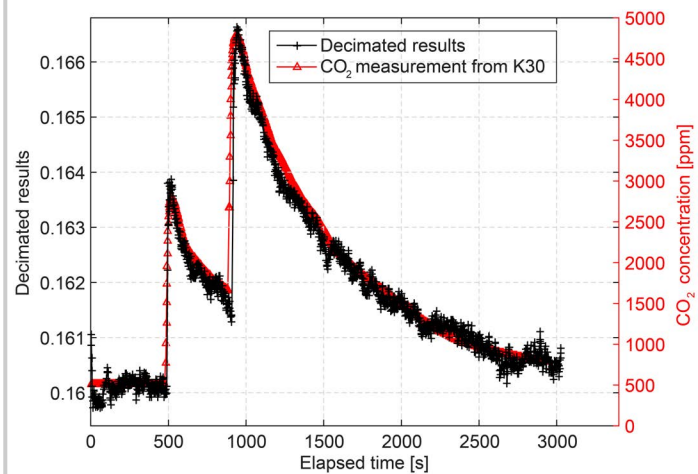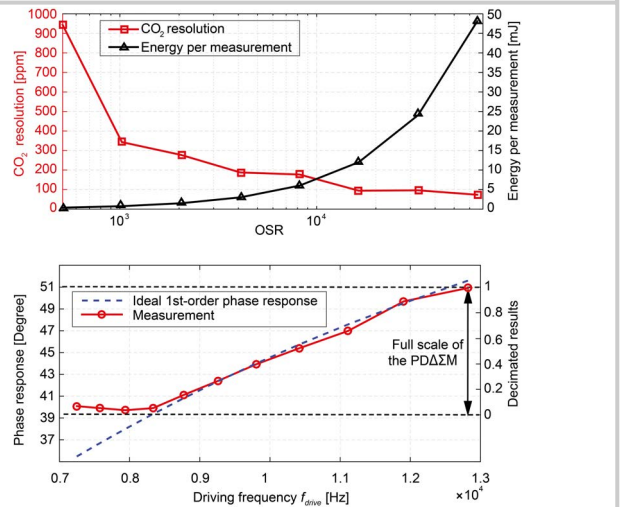**Figure 19.8.3: Circuit diagram of the proposed readout circuit.**

Figure 19.8.4: (top) Measured resolution (standard deviation of 20 consecutive measurements) and energy per measurement as a function of OSR; (bottom) measured phase shift as a function of the drive frequency.

19

Figure 19.8.5: Transient CO_2 response of the CO_2 sensor and an NDIR-based reference sensor (K30).

Parameter	This work	[3]	[2]	[1]	[6]
Method	TC	TC	TC	NDIR	NDIR
Technology	CMOS (0.16 μm)	CMOS (0.16 μm)	SOI MEMS	Module	SOI MEMS
On-chip readout	Y	Y	N	N	N
Area (sensor)	0.3 mm²	0.6 mm²	16 mm²	-	†0.3 mm²
Area (readout)	3 mm²	3 mm²	-	-	-
Supply voltage	1.8 V	1.8 V	-	5-14 V	-
Power consumption	6.8 mW	11.2 mW	3 mW	200 mW	200 mW
Meas. time	1.8 s	30 s	60 s	2 s	2.4 s
CO_2 resolution	94 ppm	202 ppm	456 ppm	20 ppm	250 ppm
Energy / meas.	12 mJ	336 mJ	180 mJ	400 mJ	480 mJ

†Area of the IR emitter only, excluding 80-mm light tube and an IR detector

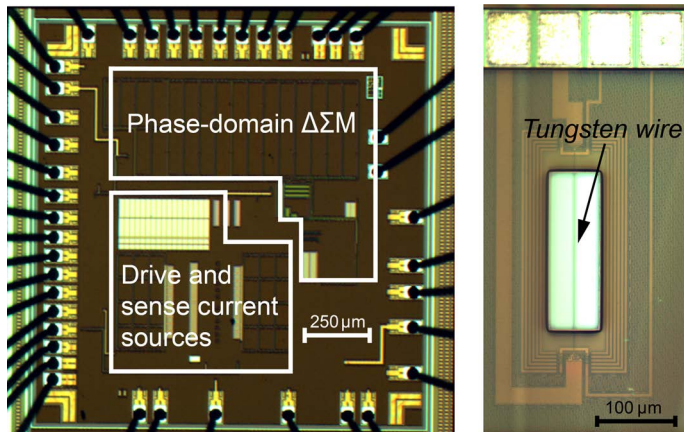**Figure 19.8.6: Performance summary and benchmarking.**

Figure 19.8.7: Die micrograph of the readout circuit and the transducer.